Rotation dynamics of coupled NTMs

Benjamin John Tobias
Princeton Plasma Physics Laboratory

with M. Chen[1], C.W. Domier[1], R. Fitzpatrick[2],
B.A. Grierson[3], N.C. Luhmann, Jr.[1],
M. Okabayashi[3], K.E.J. Oloffson[4],
C. Paz-Soldan[4], and the DIII-D team

[1]*University of California at Davis*
[2]*University of Texas at Austin*
[3]*Princeton Plasma Physics Laboratory*
[4]*General Atomics*

TSD Workshop
Princeton, NJ
July 13th, 2015

- **On DIII-D, multiple core tearing instabilities are often observed at elevated β_N**
- **Coupling amongst multiple modes has a nonlinear impact on rotation and stability**

- **At least 2 regimes of MHD-induced momentum transport can be observed in non-disruptive, Hybrid scenario discharges:**
  - Phase-locking (flattens core rotation)
  - Hollowing (flow shear reversal)

Phase-locking precedes mode locking

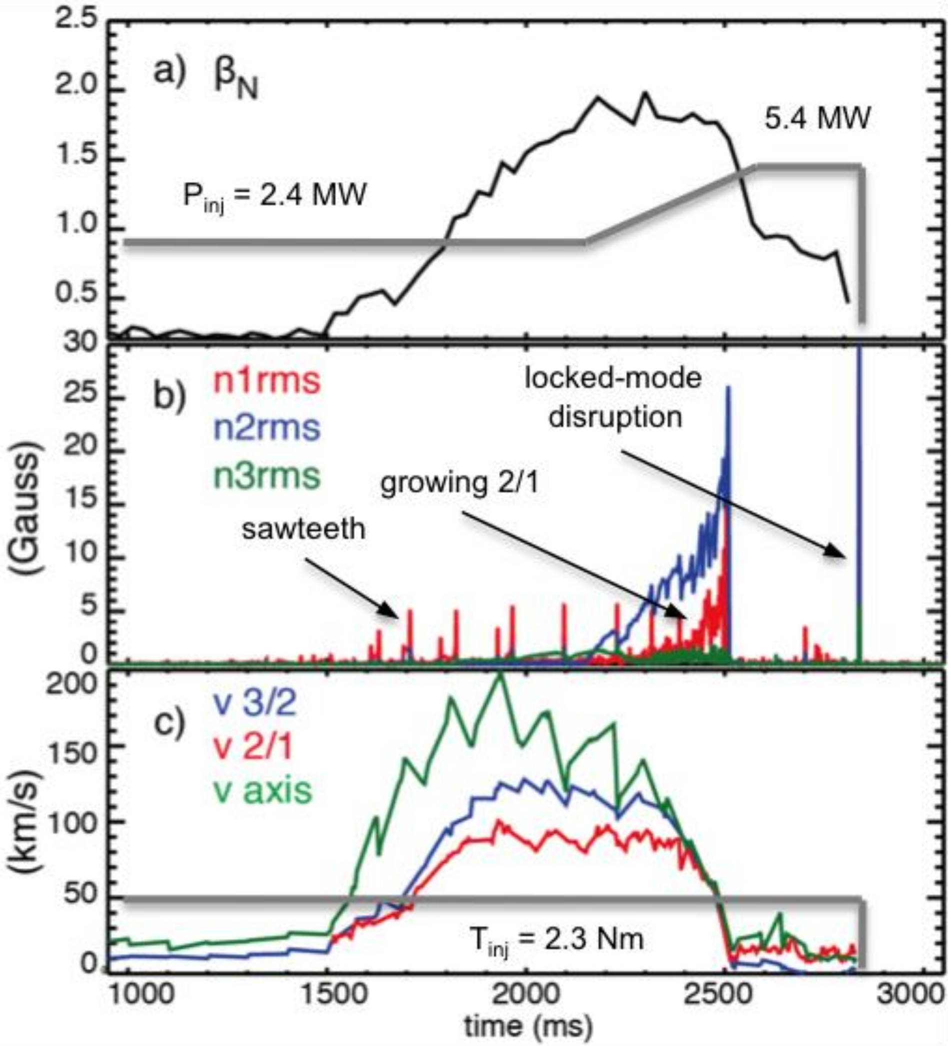

- **Growing modes trigger NBI feedback**
- **Rotation collapses from the core outward**
- **The discharge ultimately decelerates as a rigid body**

Differential rotation closely tied to disruptivity

- **Low *absolute* rotation can be sustained, but loss of *differential* rotation indicates trouble**
  - Rotation shear is classically stabilizing
  - Differential rotation decouples surfaces

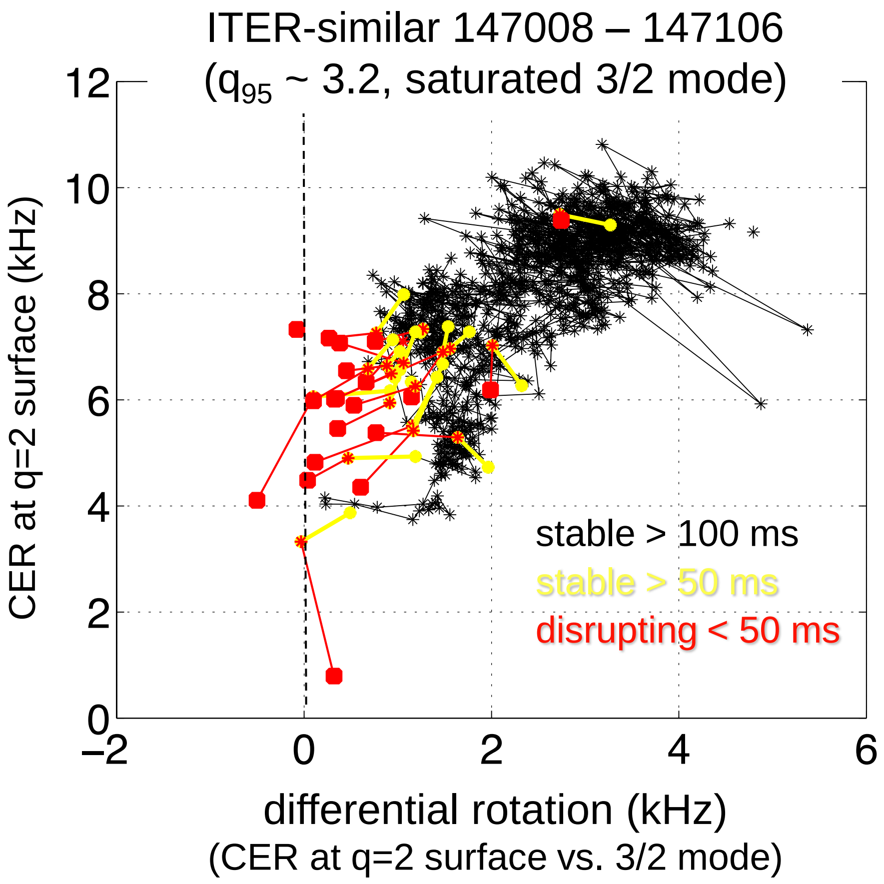

Phase-locking and rigid deceleration

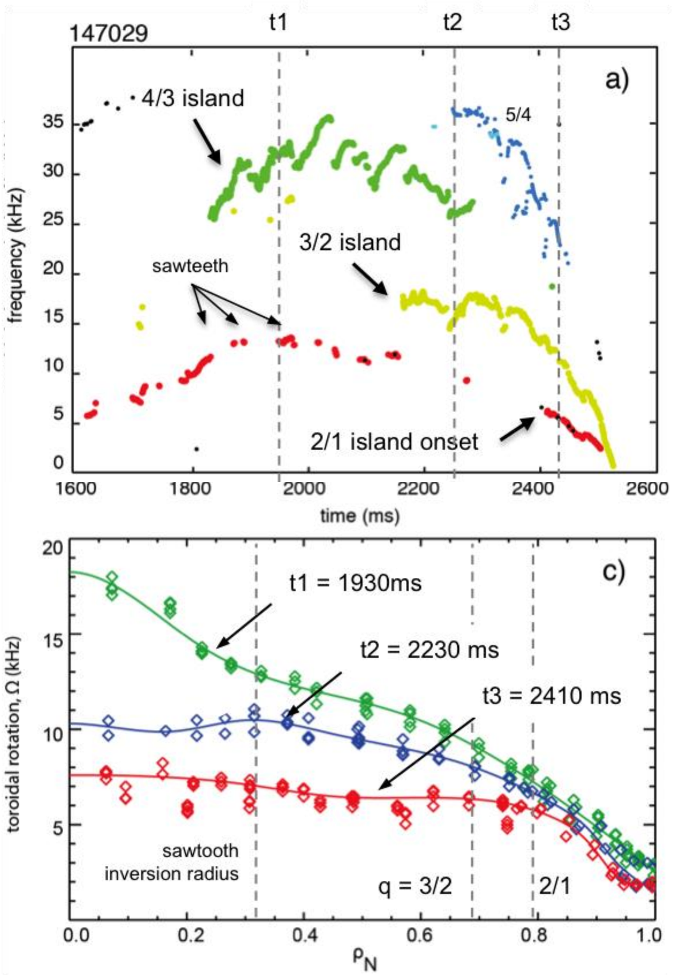

- **Mode spectra evolve toward phase-locking (toroidal co-rotation)**
- **Rotation collapses first in the core (large momentum diffusivity)**
- **2/1 mode is not triggered until the core becomes a rigid body**

Phase-locking and rigid deceleration

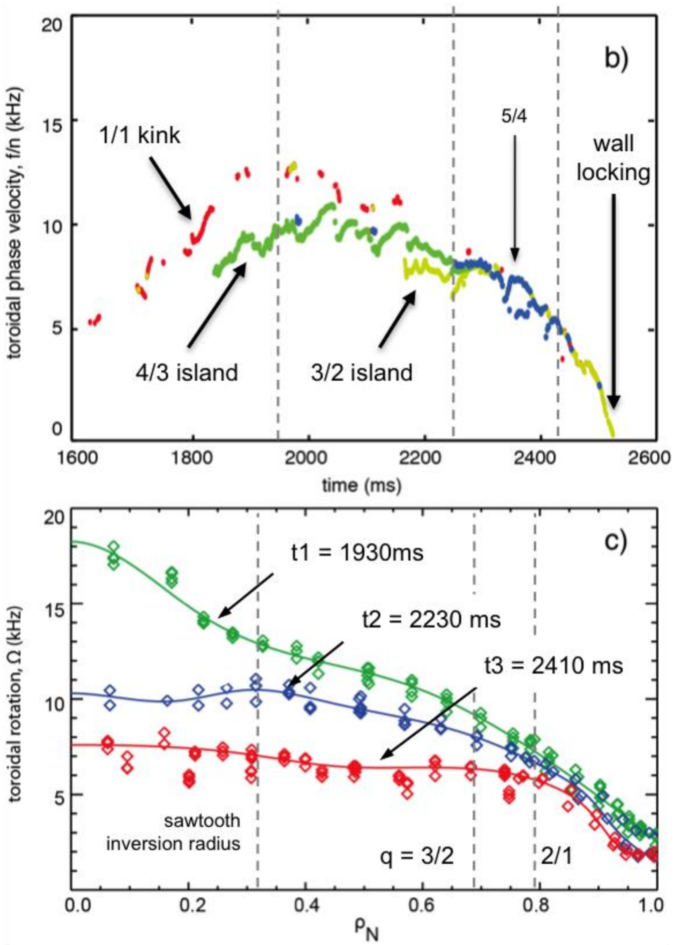

- Mode spectra evolve toward phase-locking (toroidal co-rotation)
- Rotation collapses first in the core (large momentum diffusivity)
- 2/1 mode is not triggered until the core becomes a rigid body

Phase-locking explored in non-disruptive discharges—ITER hybrid scenario on DIII-D

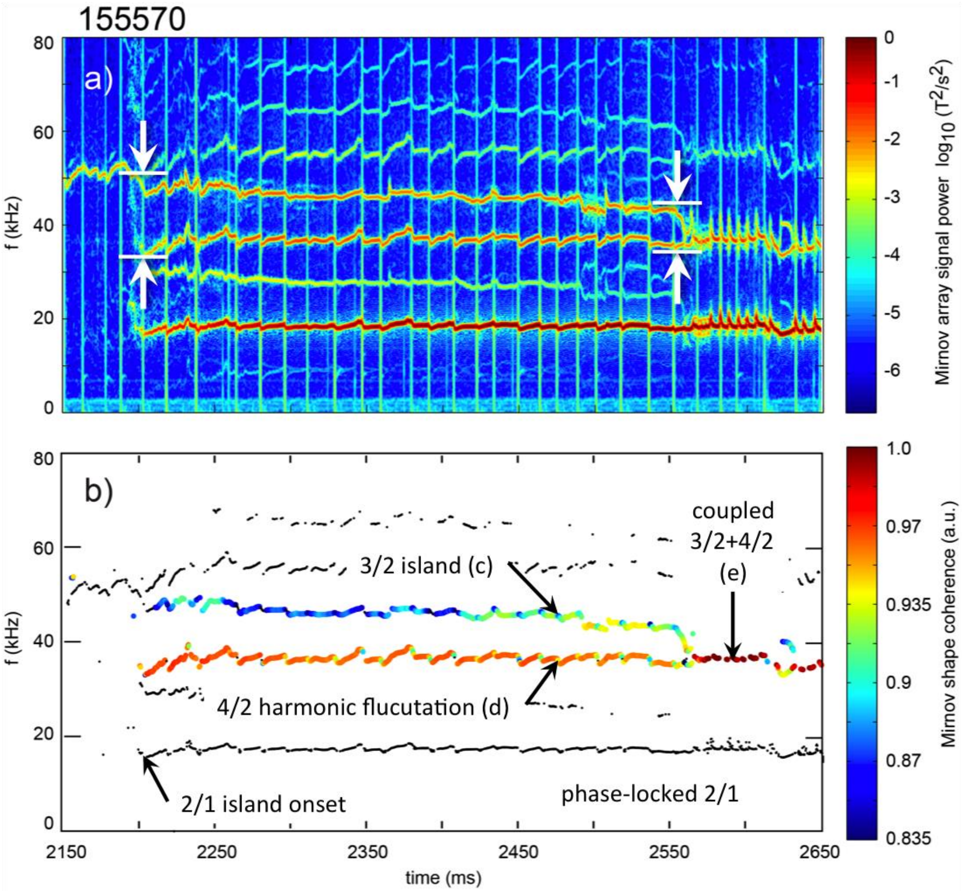

- **Modes initially rotate freely**
- **Sudden bifurcation to phase-locking**
  - Sometimes briefly ‘unlocked’ by ELMs
- **Modes saturate and discharges survive to normal shutdown**

3-wave mode coupling: the RFP ‘slinky mode’

- **Single-helicity modes couple through the Shafranov shift**
- **Single-fluid model of 3-wave coupling describes salient features:**
  - Bifurcation of torque balance
  - Phase-locking

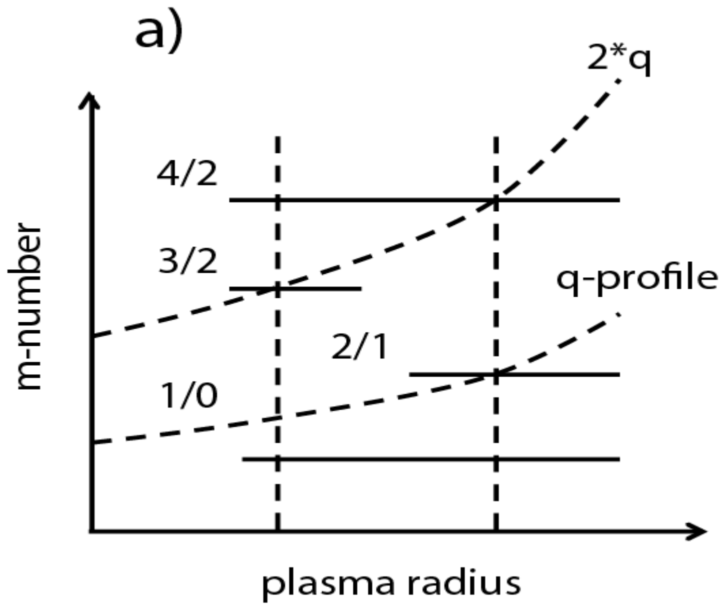

$$DY_{2,1} = EY_{2,1} + C\langle Y_{2,1}, Y_{2,1}, Y_{4,2}\rangle$$

$$DY_{3,2} = EY_{3,2} + C\langle Y_{1,0}, Y_{3,2}, Y_{4,2}\rangle$$

$$DY_{4,2} = EY_{4,2} + C\langle Y_{2,1}, Y_{2,1}, Y_{4,2}\rangle + C\langle Y_{1,0}, Y_{3,2}, Y_{4,2}\rangle$$

R. Fitzpatrick, PoP (2015)

3-wave mode coupling: the RFP ‘slinky mode’

- **Single-helicity modes couple through the Shafranov shift**
- **Single-fluid model of 3-wave coupling describes salient features:**
  - Bifurcation of torque balance
  - Phase-locking

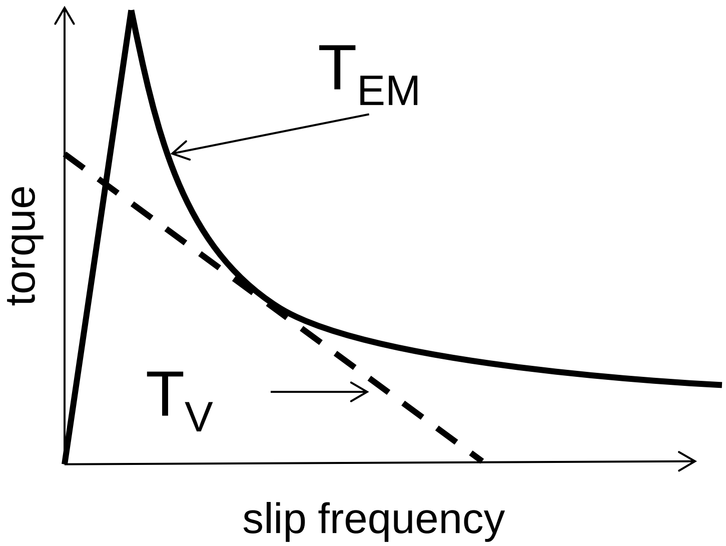

$$\Delta T^{EM}_{m,n} = \frac{2\pi^2 B_\phi^2 a^4 n}{\mu_0 R_0} \mathrm{Im}\left[\Delta\Psi_{m,n}\Psi^*_{m,n}\right]$$

$$\Delta T^{V}_{m,n} = 4\pi^2 R_0^3 \left[\mu r \frac{\partial}{\partial r}\left(\Delta\Omega_\phi\right)\right]_{r^-_{m,n}}^{r^+_{m,n}}$$

R. Fitzpatrick, PoP (2015)

3-wave mode coupling: the RFP 'slinky mode'

- **Single-helicity modes couple through the Shafranov shift**
- **Single-fluid model of 3-wave coupling describes salient features:**
  - Bifurcation of torque balance
  - Phase-locking

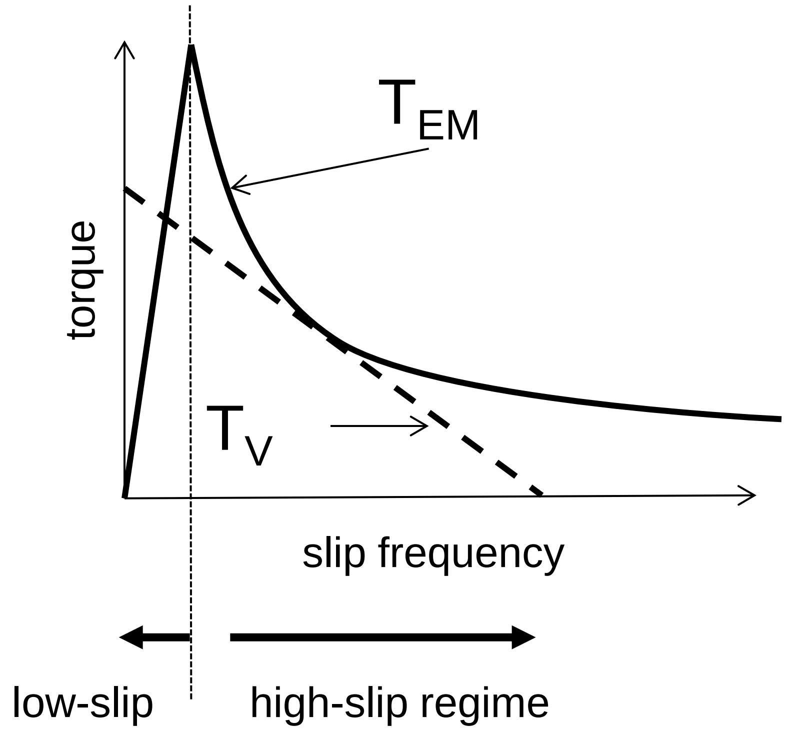

$$w_{bifurcation} = w_0 / 2$$

3-wave mode coupling: the RFP 'slinky mode'

- **Single-helicity modes couple through the Shafranov shift**
- **Single-fluid model of 3-wave coupling describes salient features:**
  - Bifurcation of torque balance
  - Phase-locking

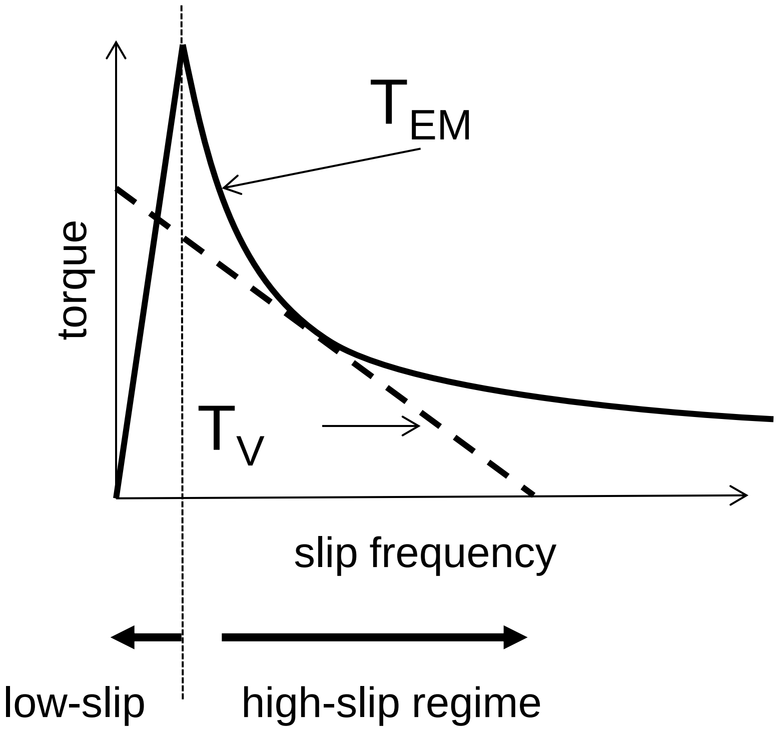

$$\delta\hat{T}_{\rm EM} = \frac{\mathcal{B}}{q_a^2}\left(w^{2m-1,2n}\right)^2\left(w^{m,n}\right)^4 \sin\varphi.$$

Internal geometry of the 'tokamak slinky:'

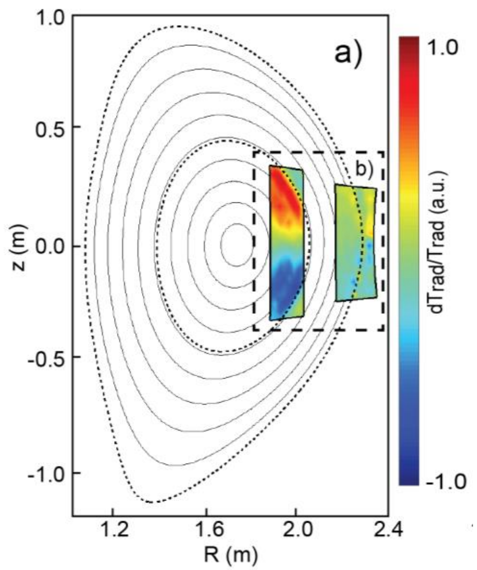

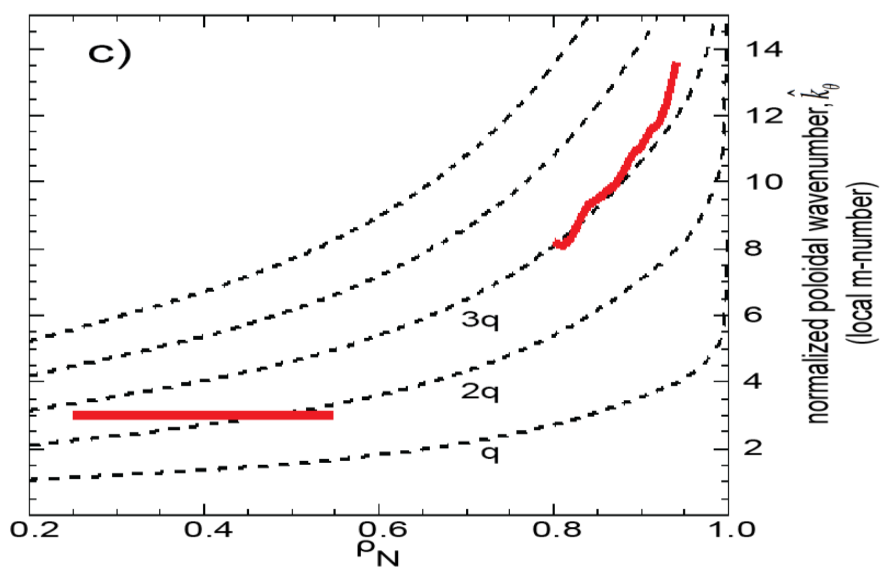

- **Mode-coupling theory developed in a cylinder, mode structure in a tokamak very different**
  - How does this impact the physics?
  - How does it modify the experimental observables?

Outer layer approximated by parameterization of local poloidal perturbation wavenumber

Contours of constant eigenmode phase

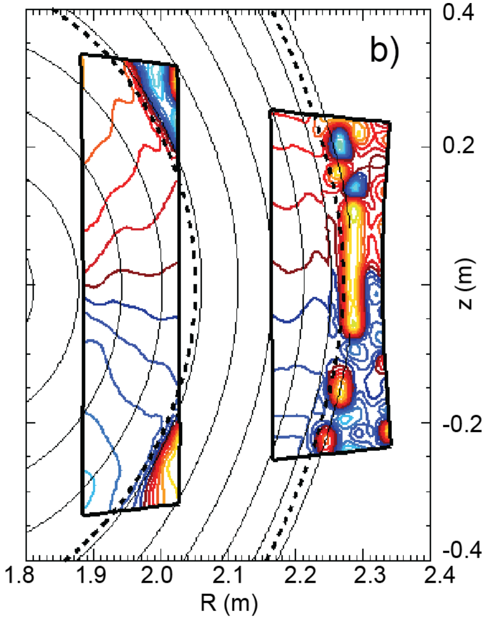

Experiment

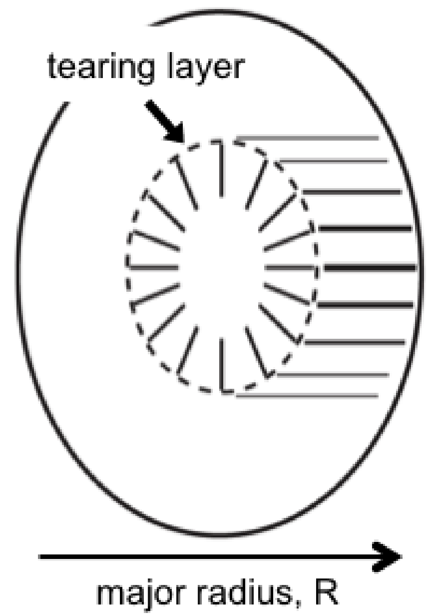

Model

Fitted 'local mode number'

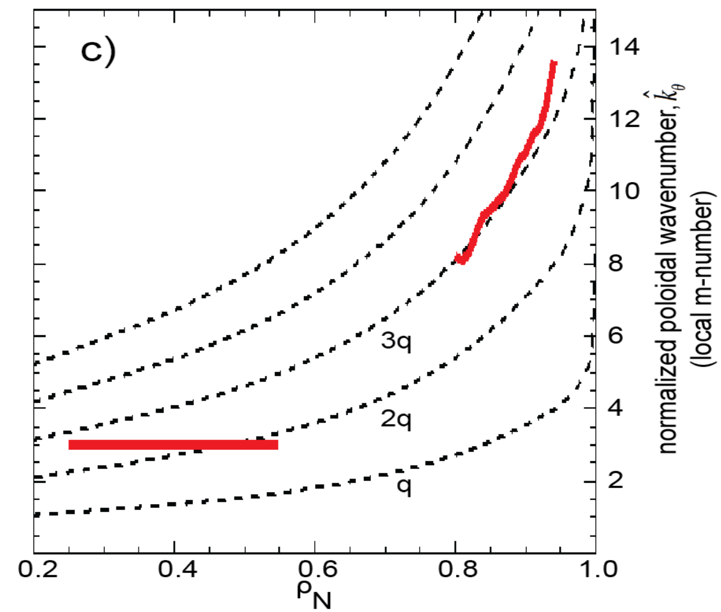

$$\hat{k}_{q0}(r)\ \mathrm{o}\ m\frac{r}{r_0},\quad R\ {}^{3}\ R_0$$

Tobias—July, 2015

Expands upon single-helicity mode spectrum by encompassing additional features

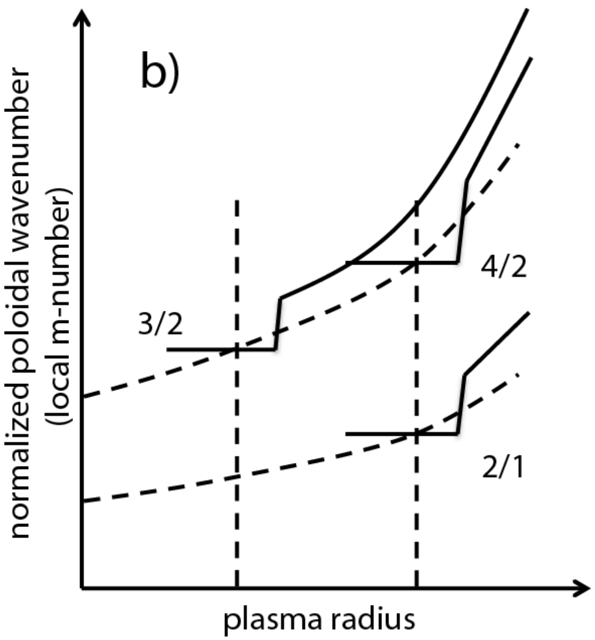

Two modes:

$$n_1 = \alpha n_0$$

$$\hat{k}_{q1} = \alpha \hat{k}_{q0} + \varepsilon$$

Become resonant when:

$$\alpha m_0 / m_1 = r_0 / r_1$$

$$r_0 / r_1 = 4/3$$

Otherwise:

$$\varepsilon(r) = \hat{k}_{q1}(r) - \alpha \hat{k}_{q0}(r) = r \left[\frac{m_1}{r_1} - \frac{\alpha m_0}{r_0} \right], \quad r \geq r_0$$

Coupling of Shafranov shift no longer explicit

Single-helicity modes in cylinder

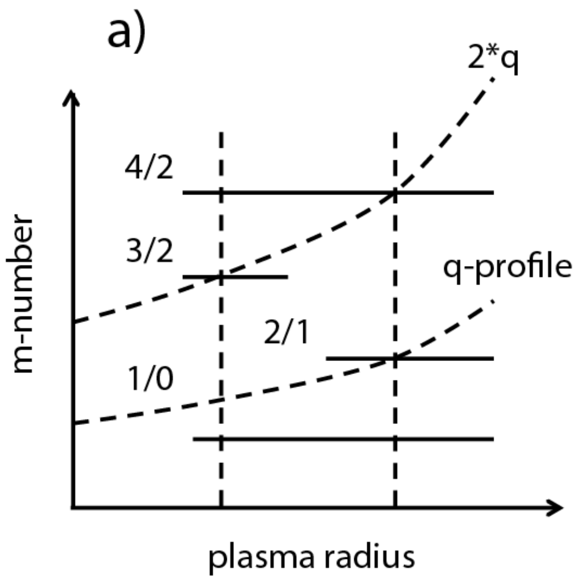

Generalized toroidal modes

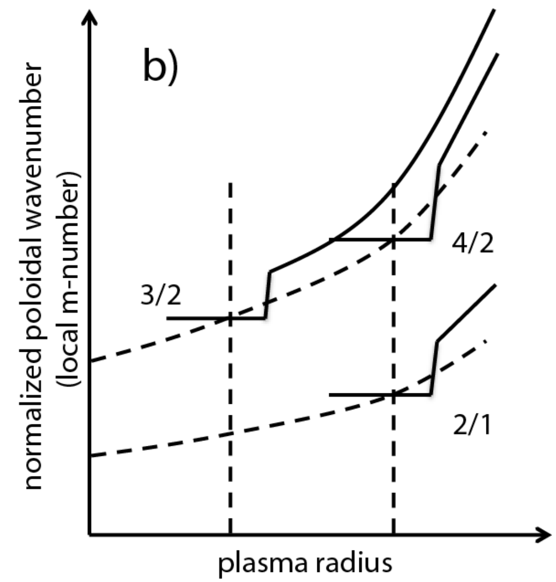

$$DY_{2,1} = EY_{2,1} + C\left\langle Y_{2,1}, Y_{2,1}, Y_{4,2}\right\rangle$$

$$DY_{3,2} = EY_{3,2} + C\left\langle Y_{1,0}, Y_{3,2}, Y_{4,2}\right\rangle$$

$$DY_{4,2} = EY_{4,2} + C\left\langle Y_{2,1}, Y_{2,1}, Y_{4,2}\right\rangle + C\left\langle Y_{1,0}, Y_{3,2}, Y_{4,2}\right\rangle$$

$$DY_{2,1} = EY_{2,1} + C\left\langle Y_{2,1}, Y_{2,1}, Y_{4,2}\right\rangle + C'\left\langle Y_{2,1}, Y_{2,1}, Y_{3,2}\right\rangle$$

$$DY_{3,2} = EY_{3,2} + C'\left\langle Y_{2,1}, Y_{2,1}, Y_{3,2}\right\rangle + D'\left\langle Y_{3,2}, Y_{4,2}\right\rangle$$

$$DY_{4,2} = EY_{4,2} + C\left\langle Y_{2,1}, Y_{2,1}, Y_{4,2}\right\rangle + D'\left\langle Y_{3,2}, Y_{4,2}\right\rangle$$

This parameterization also yields observable phase velocities (cylindrical torus)

Any given mode:

$$\mathbf{v} = \mathbf{V}\Omega = \begin{bmatrix} v_{pf} \\ v_{pq} \end{bmatrix} = \begin{bmatrix} R & -R\dfrac{\hat{k}_q}{n} \\ -r\dfrac{n}{\hat{k}_q} & r \end{bmatrix} \begin{bmatrix} W_f \\ W_q \end{bmatrix}$$

Two modes on any one, given surface:

$$\begin{bmatrix} Dv_{pf} \\ Dv_{pq} \end{bmatrix} = \begin{bmatrix} R & -R\dfrac{a\hat{k}_{q0}+e}{an_0} \\ -r\dfrac{an_0}{a\hat{k}_{q0}+e} & r \end{bmatrix} \begin{bmatrix} W_{f1} \\ W_{q1} \end{bmatrix} - \begin{bmatrix} R & -R\dfrac{\hat{k}_{q0}}{n_0} \\ -r\dfrac{n_0}{\hat{k}_{q0}} & r \end{bmatrix} \begin{bmatrix} W_{f0} \\ W_{q0} \end{bmatrix}$$

Comparing the rotation of two rational surfaces:

$$\begin{bmatrix} Dv^s_{pf} \\ Dv^s_{pq} \end{bmatrix} = \begin{bmatrix} R_1 & -R_0 \\ -r_1\dfrac{n_1}{m_1} & r_0\dfrac{n_0}{m_0} \end{bmatrix} \begin{bmatrix} W_{f1} \\ W_{f0} \end{bmatrix} - \begin{bmatrix} R_1\dfrac{m_1}{n_1} & -R_0\dfrac{m_0}{n_0} \\ -r_1 & r_0 \end{bmatrix} \begin{bmatrix} W_{q1} \\ W_{q0} \end{bmatrix}$$

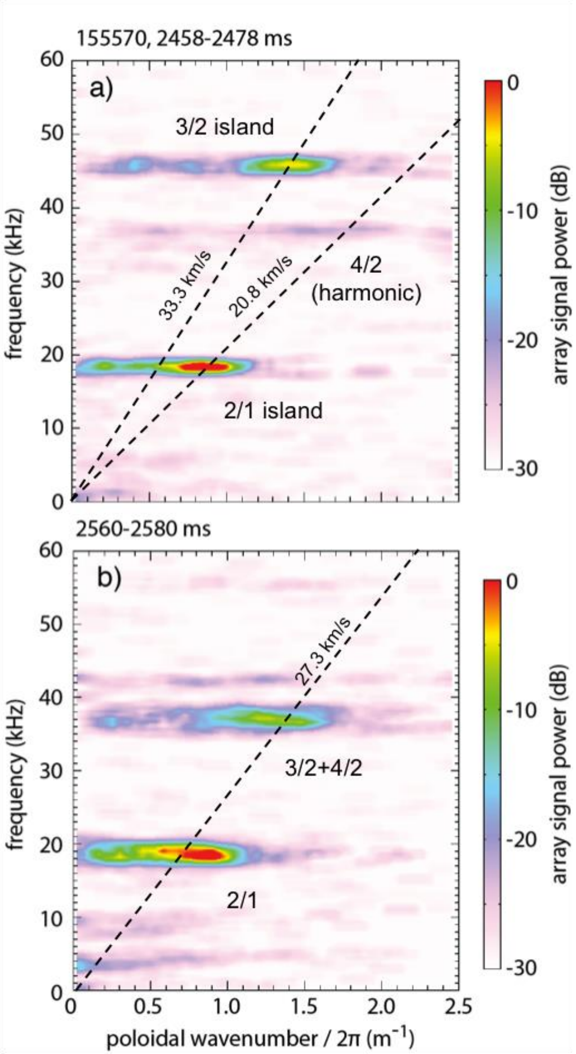

This parameterization also yields observable phase velocities (cylindrical torus)

Singular matrices

Any given mode:

$$\mathbf{v} = \mathbf{V}\Omega = \begin{bmatrix} v_{pf} \\ v_{pq} \end{bmatrix} = \begin{bmatrix} R & -R\dfrac{\hat{k}_q}{n} \\ -r\dfrac{n}{\hat{k}_q} & r \end{bmatrix} \begin{bmatrix} W_f \\ W_q \end{bmatrix}$$

Two modes on any one, given surface:

$$\begin{bmatrix} Dv_{pf} \\ Dv_{pq} \end{bmatrix} = \begin{bmatrix} R & -R\dfrac{a\hat{k}_{q0}+e}{an_0} \\ -r\dfrac{an_0}{a\hat{k}_{q0}+e} & r \end{bmatrix} \begin{bmatrix} W_{f1} \\ W_{q1} \end{bmatrix} - \begin{bmatrix} R & -R\dfrac{\hat{k}_{q0}}{n_0} \\ -r\dfrac{n_0}{\hat{k}_{q0}} & r \end{bmatrix} \begin{bmatrix} W_{f0} \\ W_{q0} \end{bmatrix}$$

Comparing the rotation of two rational surfaces:

$$\begin{bmatrix} Dv^s_{pf} \\ Dv^s_{pq} \end{bmatrix} = \begin{bmatrix} R_1 & -R_0 \\ -r_1\dfrac{n_1}{m_1} & r_0\dfrac{n_0}{m_0} \end{bmatrix} \begin{bmatrix} W_{f1} \\ W_{f0} \end{bmatrix} - \begin{bmatrix} R_1\dfrac{m_1}{n_1} & -R_0\dfrac{m_0}{n_0} \\ -r_1 & r_0 \end{bmatrix} \begin{bmatrix} W_{q1} \\ W_{q0} \end{bmatrix}$$

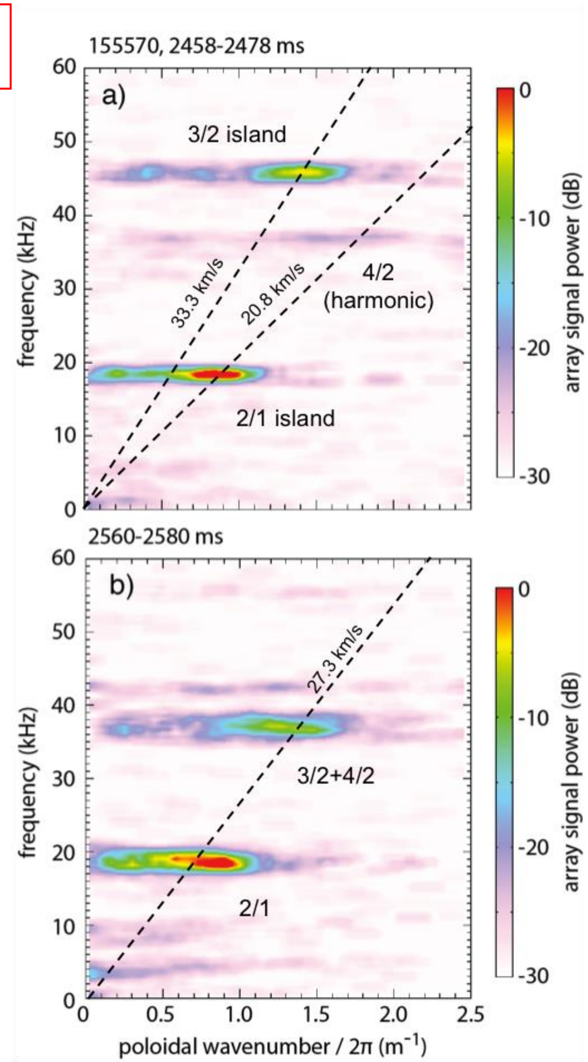

Experimental observation of phase-locking

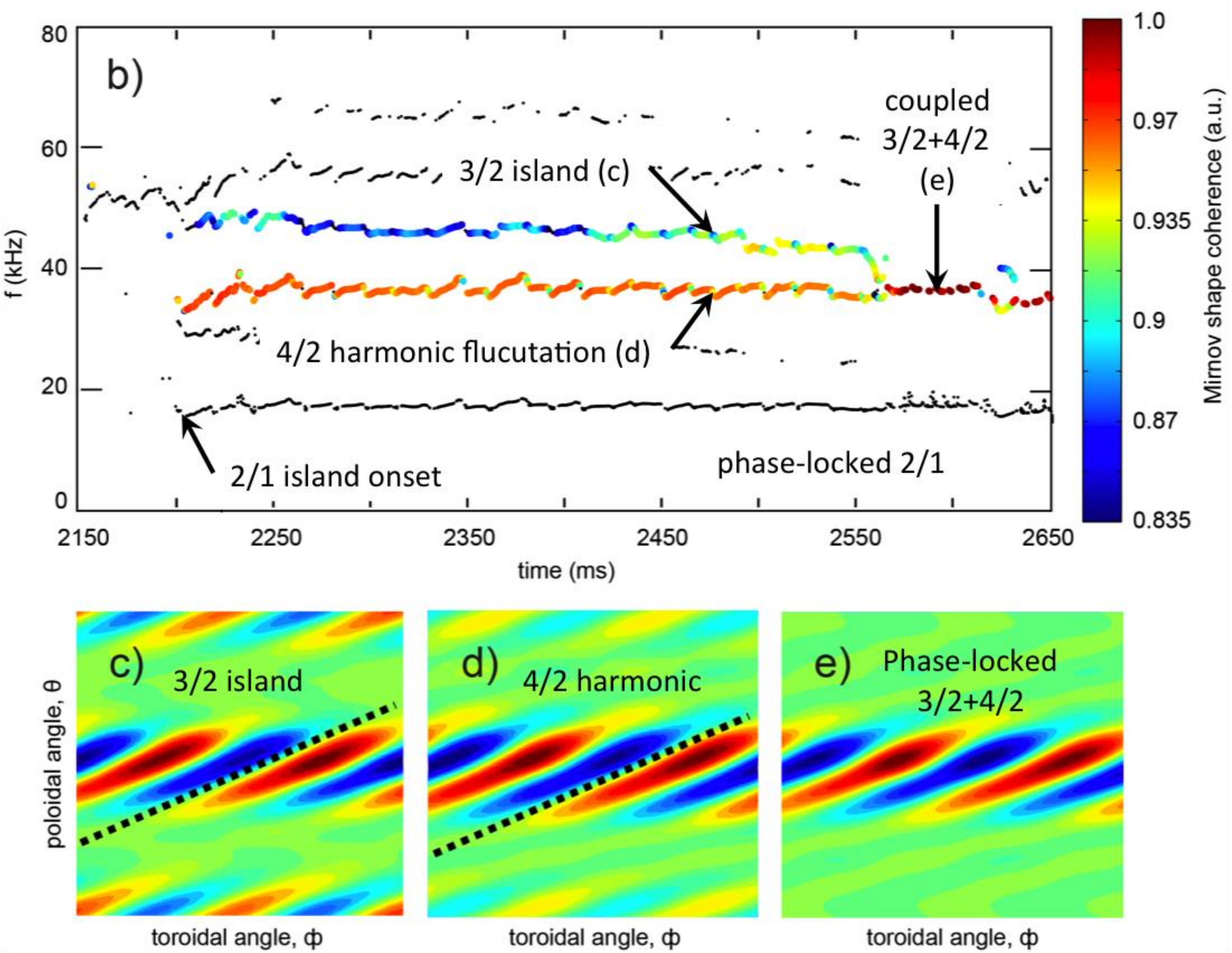

DIII-D NATIONAL FUSION FACILITY SAN DIEGO

Experimental observation of phase-locking

Conditions here controlled by q_{95}

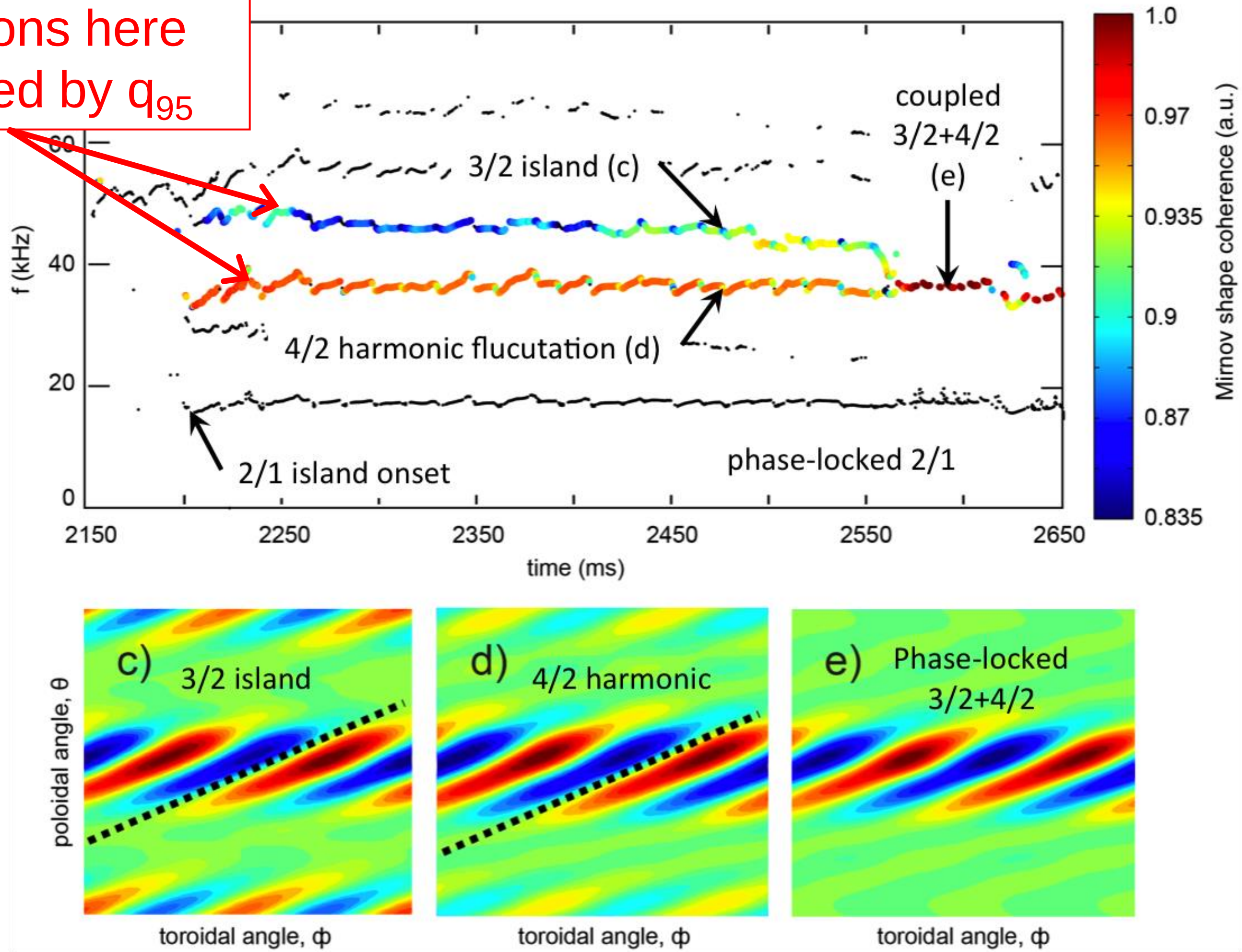

DIII-D NATIONAL FUSION FACILITY SAN DIEGO

Momentum transport increases at lower q_{95}

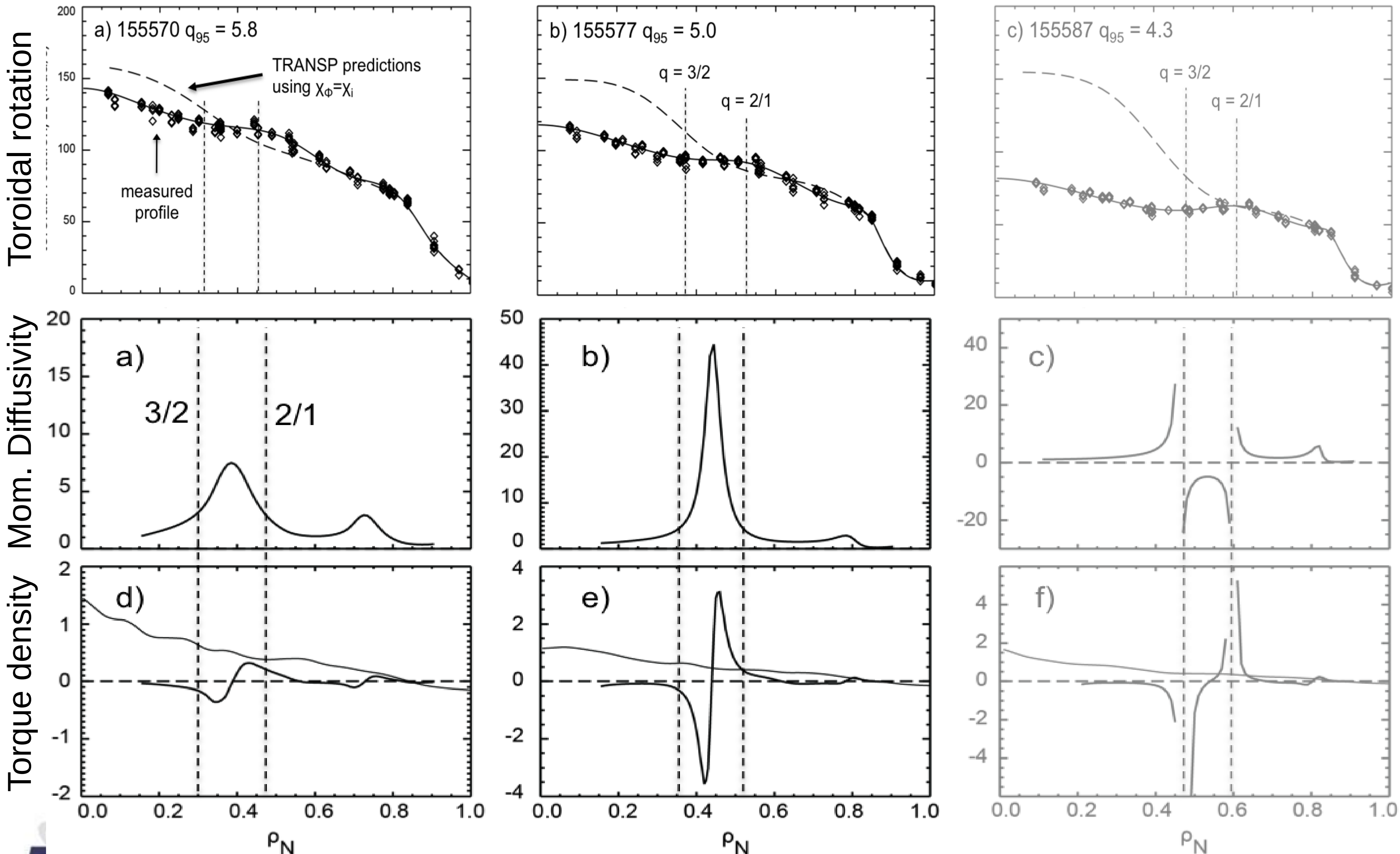

Tobias—July, 2015

NATIONAL FUSION FACILITY
SAN DIEGO

Momentum transport increases at lower q_{95}

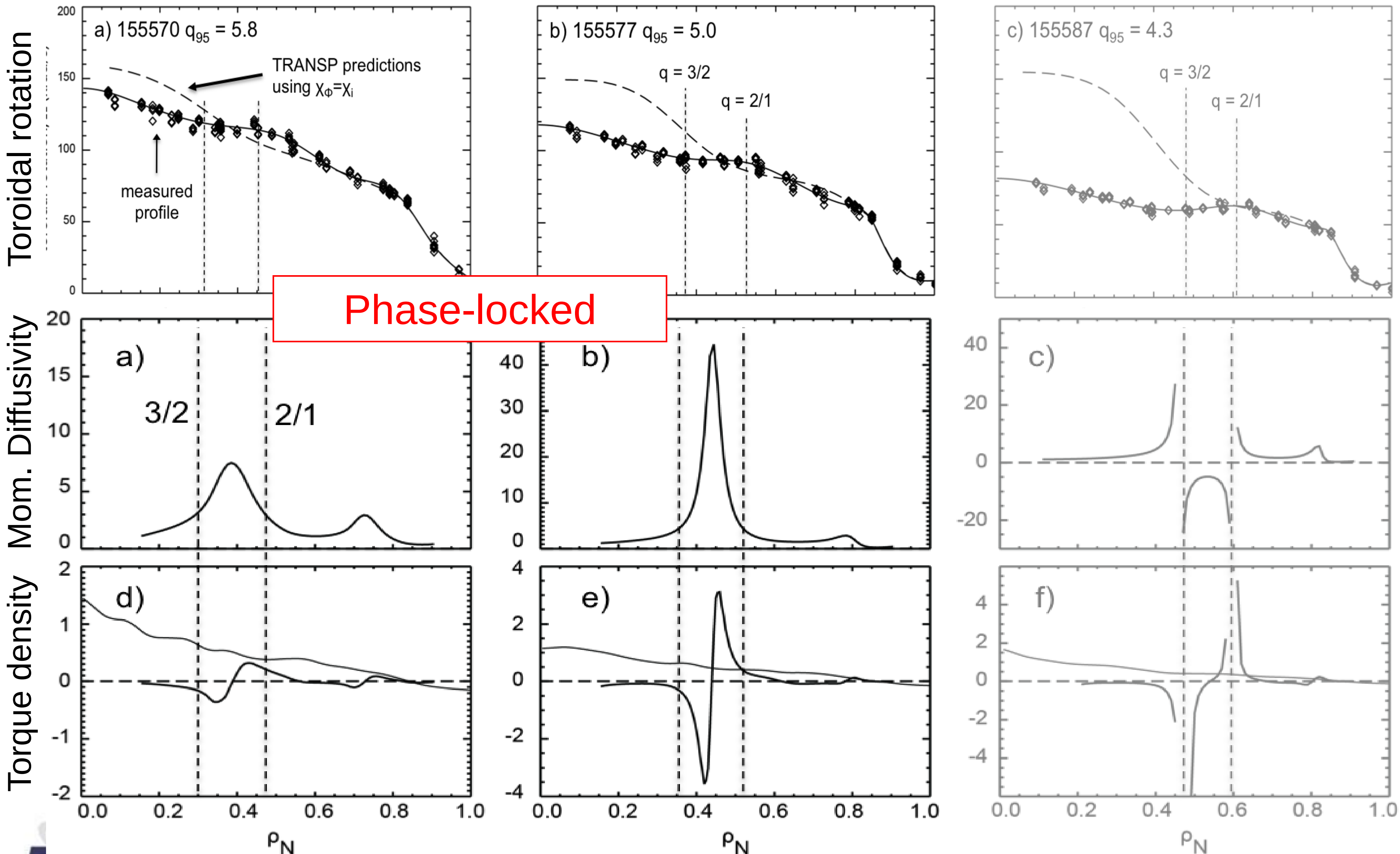

Tobias—July, 2015

Momentum convection arises at q_{95} ~ 4.5

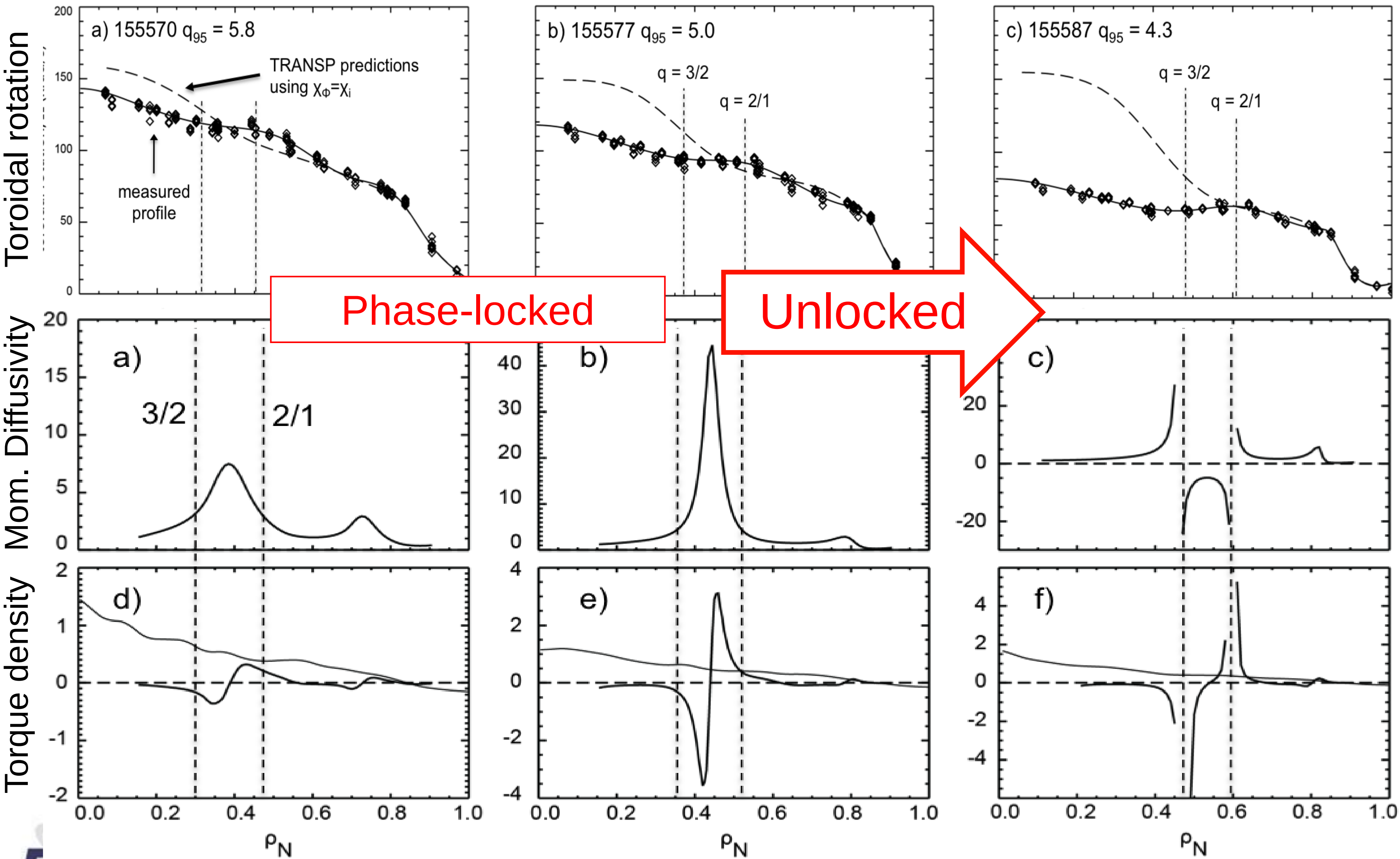

Tobias—July, 2015

Below q_{95}~4.5, modes' pitch does not align and modes do not remain phase-locked

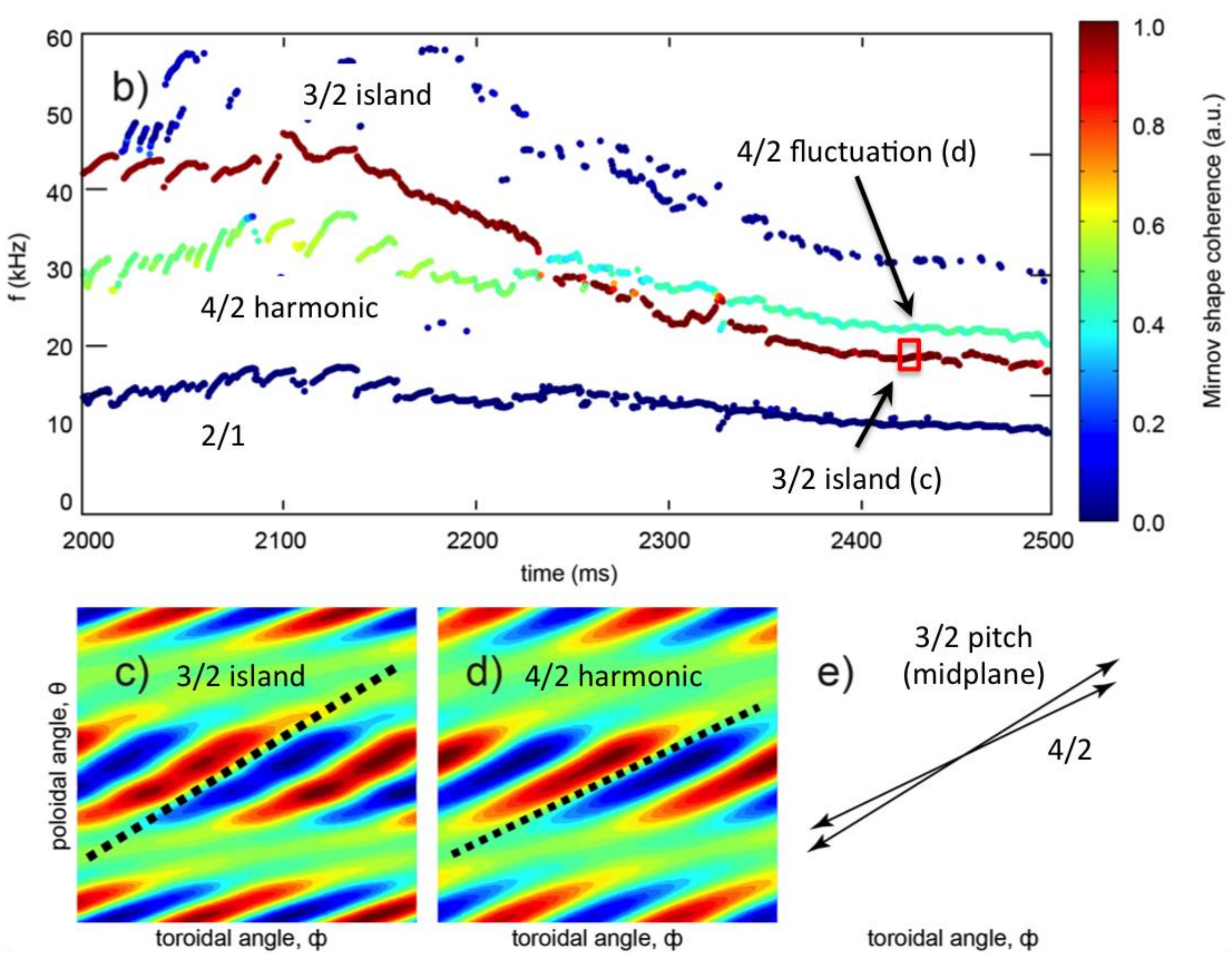

Tobias—July, 2015

Differential pitch of the modes coincides with differential toroidal and poloidal phase velocity

- **Toroidal phase velocity from Mirnov array:**

$$\Delta v_{\phi} = \frac{-R}{n_0}\frac{\epsilon}{a}\Omega_{\theta 0}$$

← *Consistent with Fitzpatrick*

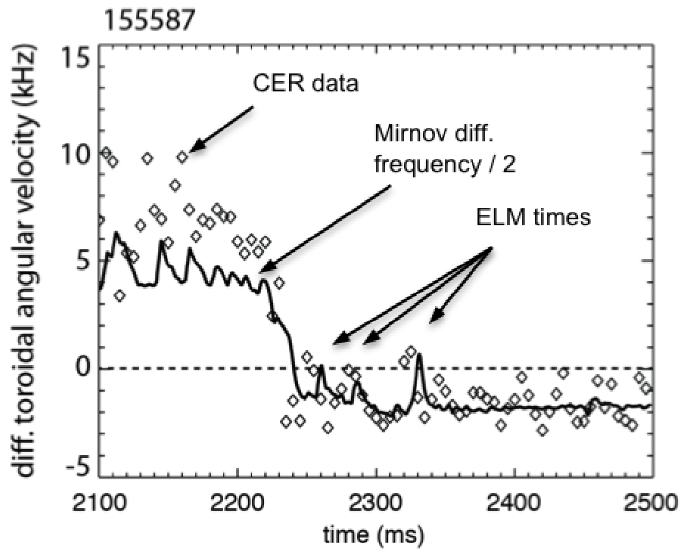

- **Poloidal phase velocity from microwave imaging:**

$$\Delta v_{\theta} = \frac{r}{k_0}\frac{\epsilon}{a}\left[\Omega_{\theta 0} - \left(\Omega_{\theta 1} - \frac{\alpha n_0}{\alpha k_0 + \epsilon}\Omega_{\phi 1}\right)\right]$$

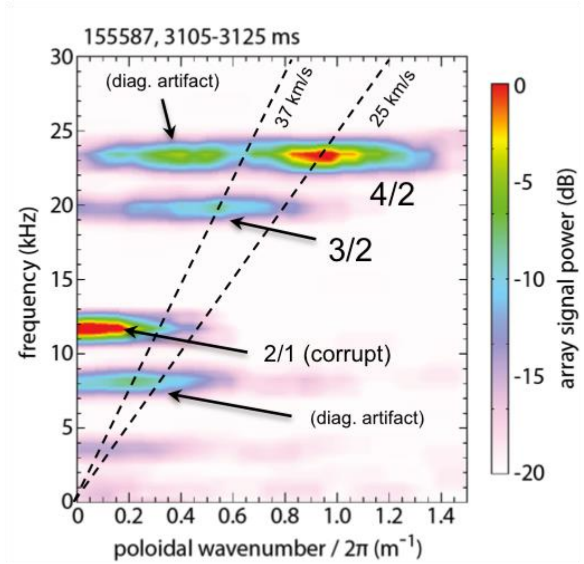

Rotation of the composite structure can be evaluated in the plasma fluid frame

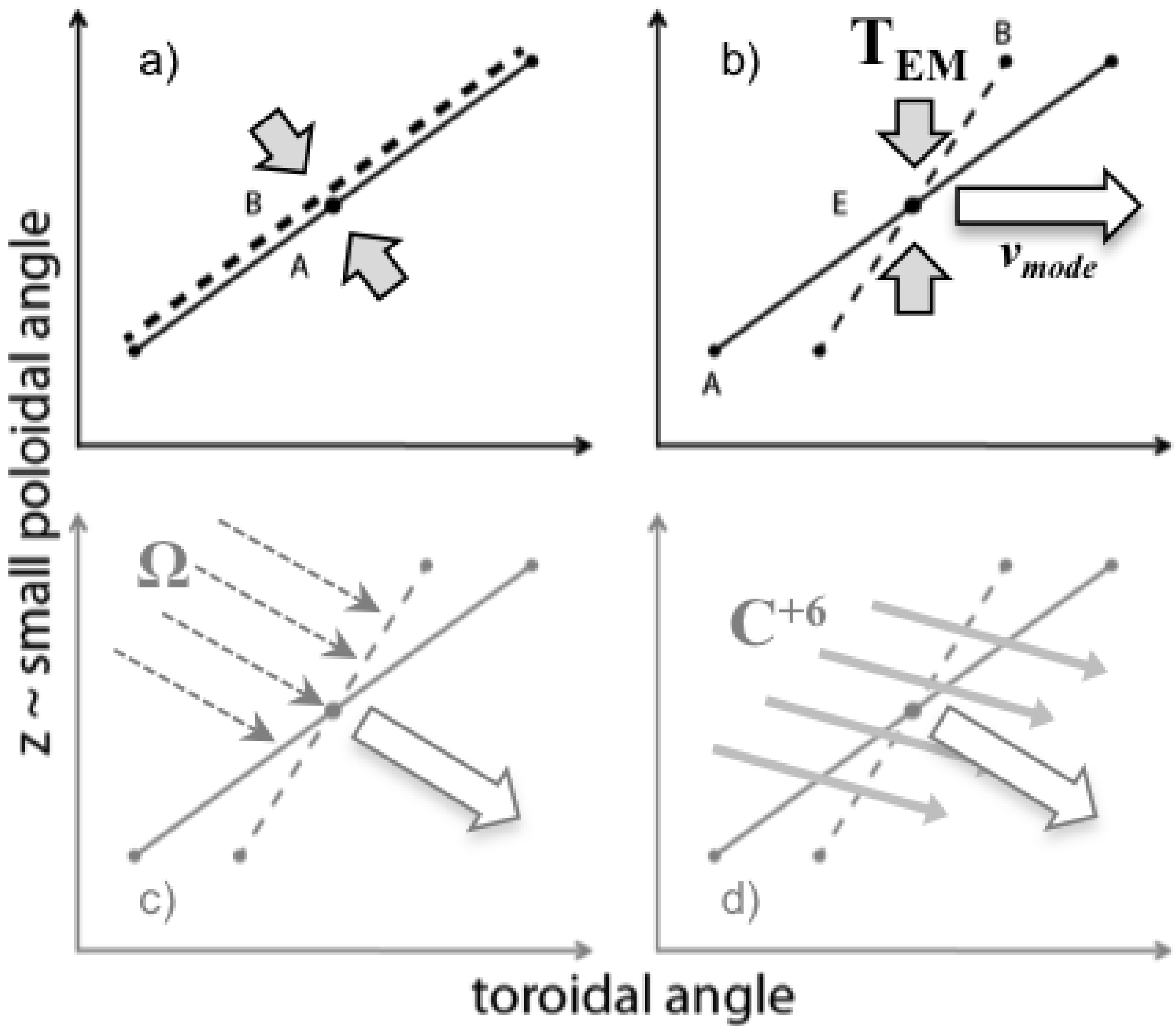

Rotation of the composite structure can be evaluated in the plasma fluid frame

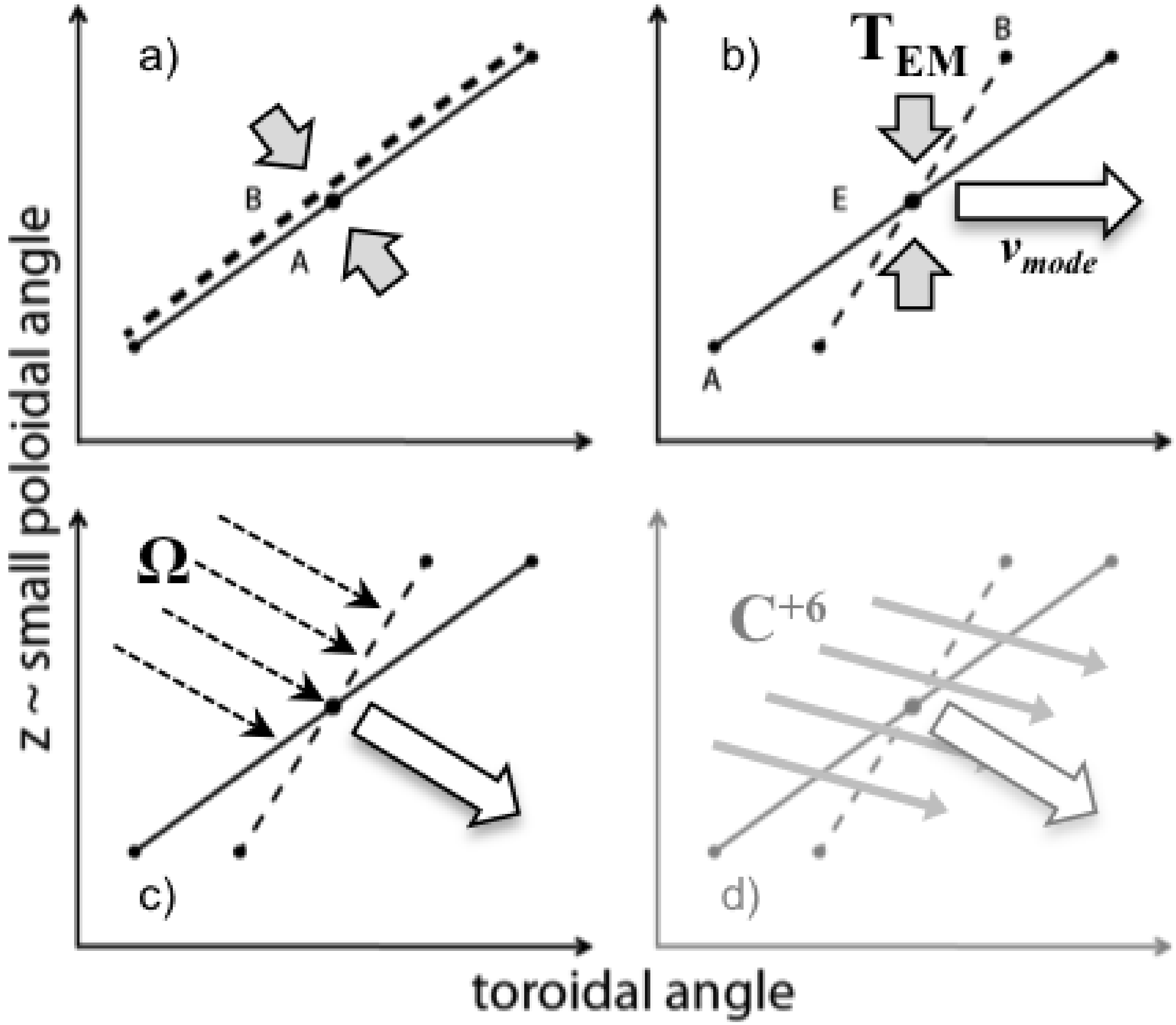

Rotation of the composite structure can be evaluated in the plasma fluid frame

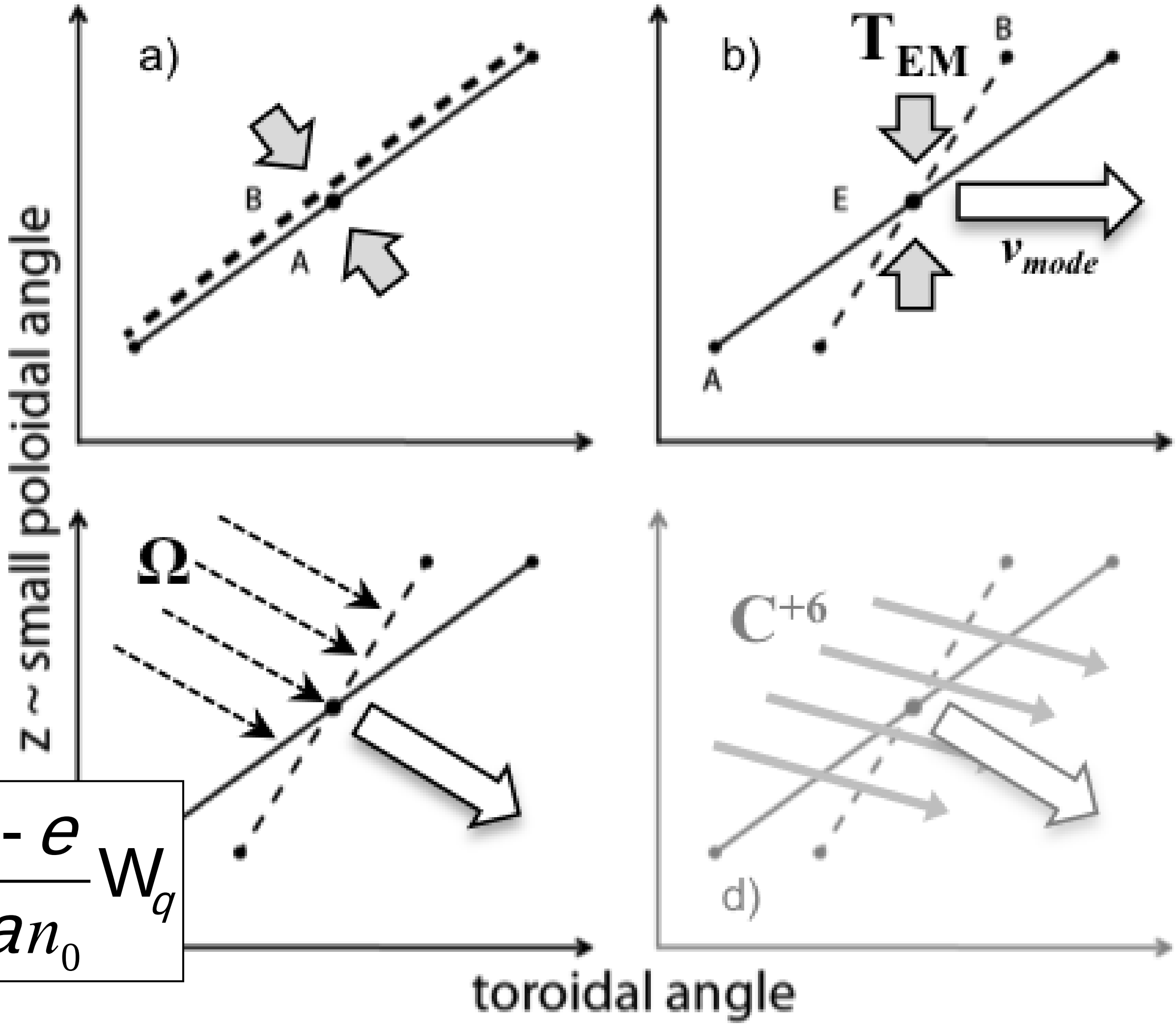

$$\frac{D v_{pf}}{R} = \frac{-e}{a n_0} W_q$$

Rotation of the composite structure can be evaluated in the plasma fluid frame

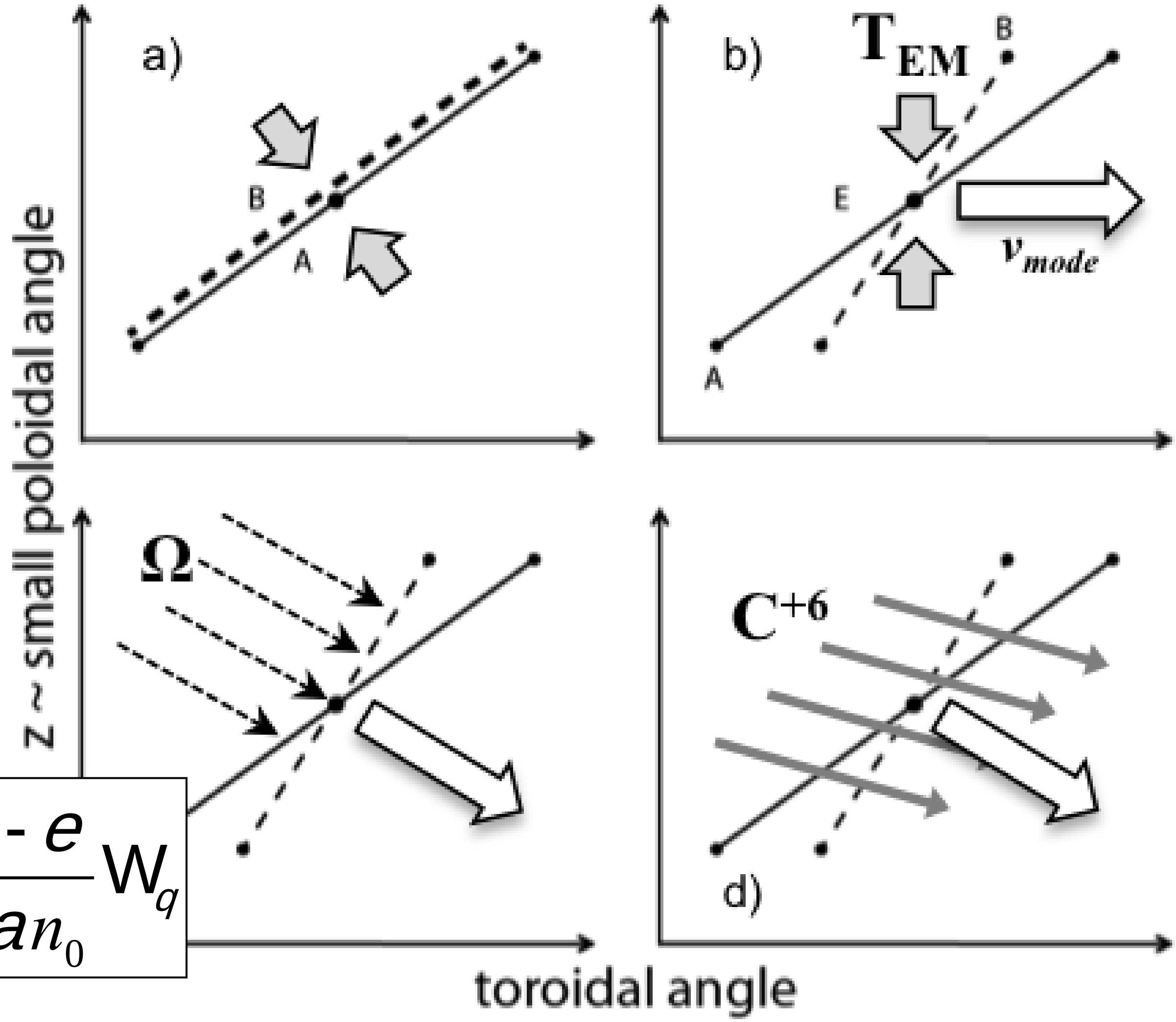

$$\frac{\Delta v_{pf}}{R} = \frac{-e}{a n_0}\Omega_\theta$$

Rotation of the composite structure can be evaluated in the plasma fluid frame

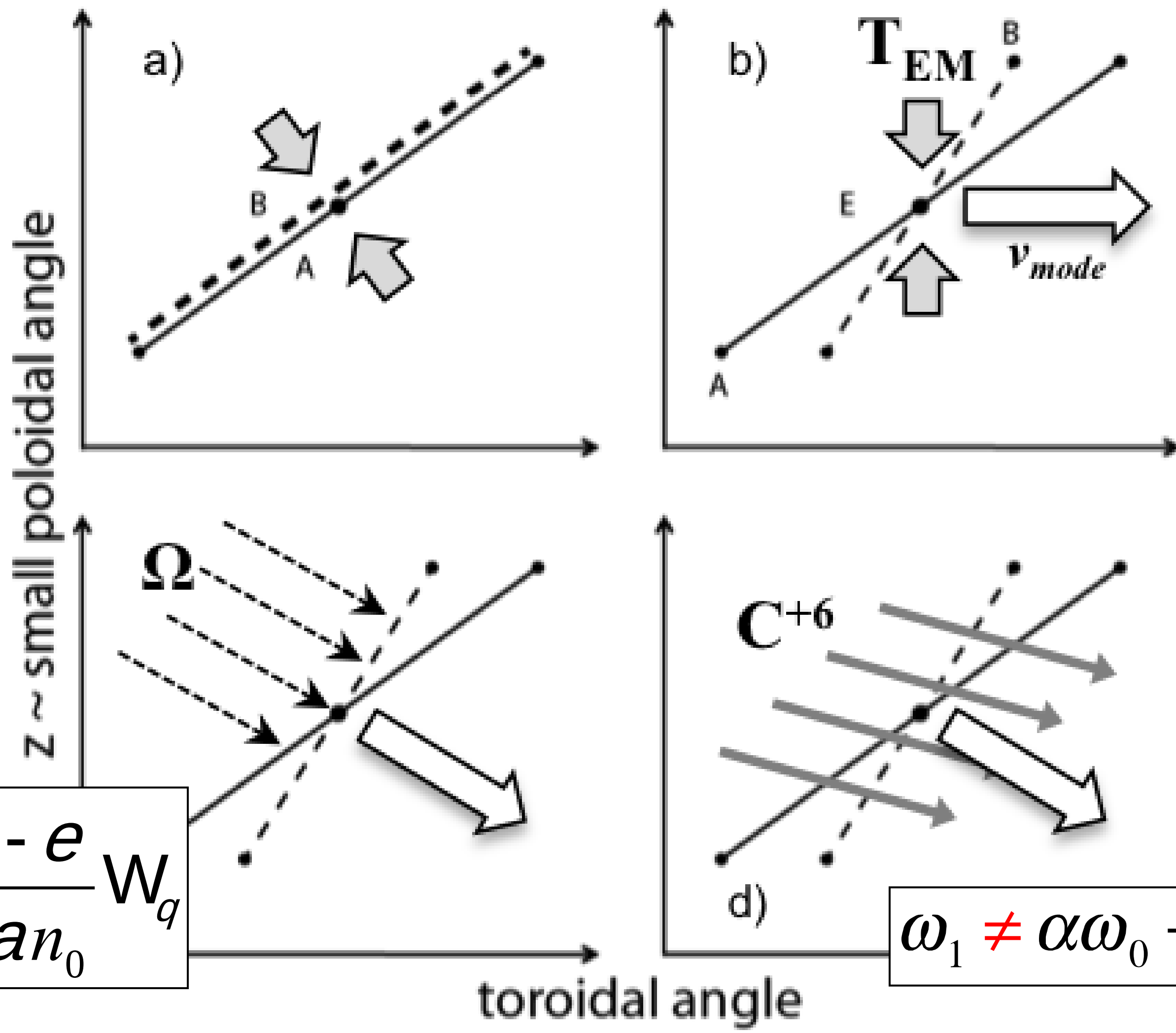

$$\frac{\Delta v_{pf}}{R} = \frac{-e}{a n_0}\Omega_\theta$$

$$\omega_1 \neq \alpha\omega_0 + \epsilon\Omega_\theta$$

Rotation of the composite structure can be evaluated in the plasma fluid frame

$$\frac{\Delta v_{pf}}{R} = \frac{-\varepsilon}{\alpha n_0}\Omega_\theta$$

Poloidal rotation can break phase-locking

$$0 = \begin{bmatrix} \left(\alpha \hat{k}_{\theta 0} + \varepsilon\right) & -\alpha n_0 \\ -\hat{k}_{\theta 0} & n_0 \end{bmatrix} \begin{bmatrix} \Delta\Omega_\theta \\ \Delta\Omega_\phi \end{bmatrix}$$

…but these modes can still be ‘co-propagating’ with the fluid on a given flux surface

$$\omega_1 = \alpha\omega_0 + \varepsilon\Omega_\theta$$

In tokamak geometry using flux-conserved rotation variables, the condition of co-propagation becomes:

$$n_1 \Delta\Omega = k_0\Gamma_0 - k_1\Gamma_1$$

$$\Gamma_j = \frac{\hat{k}_{\theta 1j} B_{\theta j}}{\rho_j} - \frac{n_1 B_{\phi j}}{R_j}$$

Poloidal rotation lags behind rotation of the combined mode structures

Toroidal Rotation

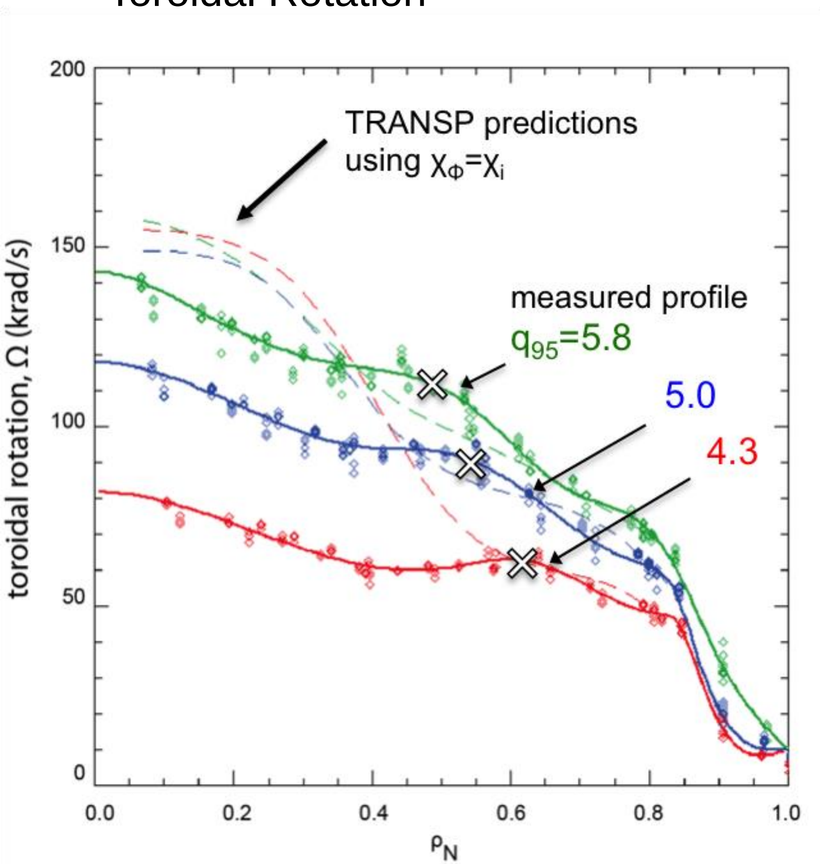

Poloidal Rotation (vertical CER)

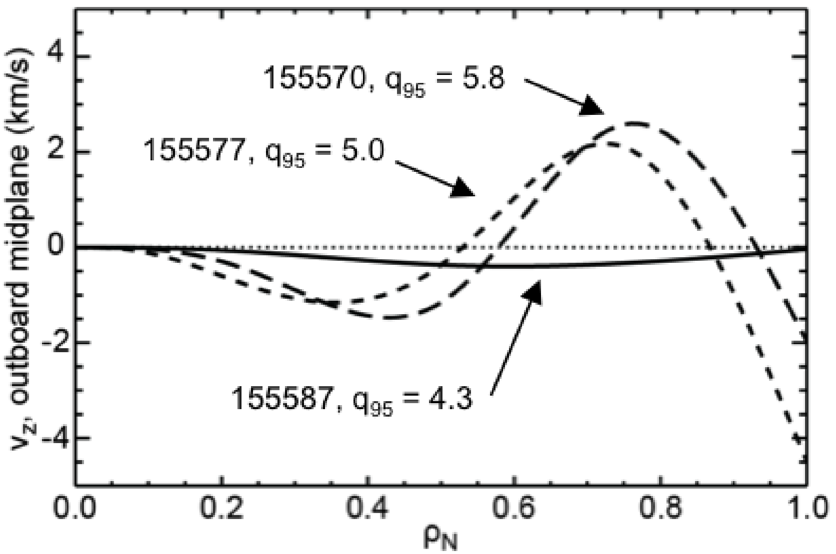

Rotation of the composite structure is ~ 5 km/s at either rational surface *(about 10x measured Carbon flow)*

DIII-D NATIONAL FUSION FACILITY SAN DIEGO

Negative differential rotation implies a regime of further non-ambipolarity

- **Points of constructive perturbation phase in the composite mode structure propagate ahead of the measured Carbon (and estimated main ion) fluid in the ion diamagnetic direction**
  - Past the point of EM force balance predicted by theory and overcoming fluid viscosity
- **Computed E_r (quasi-neutral force balance) has been reduced; *are non-ambipolar terms required?***
  - *Next avenue of investigation:*

$$E_r = v_f B_q - v_q B_f + \frac{\nabla P_i}{Z_i e n_i} + ?$$

H. Phase-Locked State

Following the analysis of Sect. IV H, the phase-locked state is characterized by $\omega = 0$, and

$$\varphi(t) = \varphi_0, \tag{197}$$

where φ_0 is a constant. Thus, Eqs. (178) and (179) yield

$$0 = -m\,\Omega_\theta^{m,n} + (m+1)\,\Omega_\theta^{m+1,n} + n\,\Omega_\phi^{m,n} - n\,\Omega_\phi^{m+1,n}, \tag{198}$$

$$0 = \omega_0 + n\,\Delta\Omega_\phi^{m,n} - n\,\Delta\Omega_\phi^{m+1,n}, \tag{199}$$

respectively. If the plasma rotates poloidally as a solid body [i.e., $\Omega_\theta(\hat{r}) = \Omega_\theta$], as is likely to be the case in the plasma core, then Eq. (198) implies that

$$\Omega_\phi^{m,n} = \Omega_\phi^{m+1,n} - \frac{\Omega_\theta}{n}. \tag{200}$$

R. Fitzpatrick, PoP (2015)